Annual Report

on

Processing $FeBO_3$ Glass-Ceramics in Space

June 25, 1975 - September 30, 1976

to

National Aeronautics and Space Administration
George C. Marshall Space Flight Center
Marshall Space Flight Center, Alabama

Contract No. NAS8-31381
DCN 1-5-58-00273 (IF)

from

Owens-Illinois, Inc.
Materials Research Section
Toledo, Ohio

by

C. T. Li

October 15, 1976

ABSTRACT

The purpose of this study is to explore the possibility of preparing $FeBO_3$ glass-ceramic in space. A transparent glass-ceramic of $FeBO_3$, due to its unique properties could be an excellent material for magneto-optic applications which currently utilize high price materials such as single crystals of Ga-YIG ($2700/lb.). The unique magneto-optic properties of $FeBO_3$ were found to come from the glass-ceramic but not from the glass form. It was anticipated and later confirmed that the $FeBO_3$ glass-ceramics could not be prepared on earth. The two terrestrial manufacturing obstacles, namely, phase separation and iron valence reduction, were identified in the study of $FeBO_3$. Since the phase separation problem could be overcome by space processing, the preparation of $FeBO_3$ glass-ceramic in space appears attractive. The iron borate composition best suited for space processing was determined to be $Fe_2O_3 \cdot 5B_2O_3$. This calculated composition is expected to form glass readily in space, because it was possible to form, although with great difficulty, a glass on earth. In addition, the prospect of producing a transparent glass in space looks good for this chosen composition, based upon a consideration of the particle size present in the glasses prepared on earth, and particularly if steps can be taken to minimize the iron reduction. However, continued work on $FeBO_3$ is deemed necessary in order to assess the prospect of producing a transparent glass-ceramic in space.

Table of Contents

List of Tables

Page

List of Figures

1. Suitability of $FeBO_3$ for space processing

The purpose of this study is to explore the possibility of preparing $FeBO_3$ glass-ceramics in space. $FeBO_3$ is a very unique material[1-5] which is transparent and ferromagnetic at room temperature and has an extremely high ratio of Faraday rotation to optical absorption (14°/dB) in the visible (5250 Å). The properties of $FeBO_3$ single crystals are summarized in Table 1. The ratio of Faraday rotation to optical absorption which is often called the figure of merit is a measure of efficiency for materials to be used in magneto-optical devices and is also one of the most important material parameters in Faraday effect devices. $FeBO_3$ would become the excellent material for magneto-optic applications, which are currently utilizing the high price material of single crystal Ga-YIG ($2700/lb.), were it not for the drawbacks associated with the current earth-prepared $FeBO_3$, i.e., it can only be prepared as single crystals and ceramic materials. The drawbacks are detailed in Table 2. It is anticipated that a transparent glass-ceramic of $FeBO_3$ not only would keep the unique properties but also should be free from such drawbacks as exist for the current earth-prepared $FeBO_3$ materials. However, it is highly unlikely that the transparent $FeBO_3$ glass-ceramics can ever be made on earth due to the high iron content (70 wt.% Fe_2O_3 in $FeBO_3$) and also due to the structure limitation making it difficult for iron borate ($FeBO_3$) to form glass. This prediction has since been confirmed by this study sponsored by NASA. Space processing will likely provide the following benefits for $FeBO_3$:

(a) Extend the range of glass forming by containerless melting.

(b) Overcome the phase separation problem on earth by near-zero gravity.

The potential commercial application makes $FeBO_3$ a good candidate material for space processing. In order to help evaluate the prospect of forming the $FeBO_3$ glass-ceramic in space, the overall plan designed for this study is schematically outlined as follows:

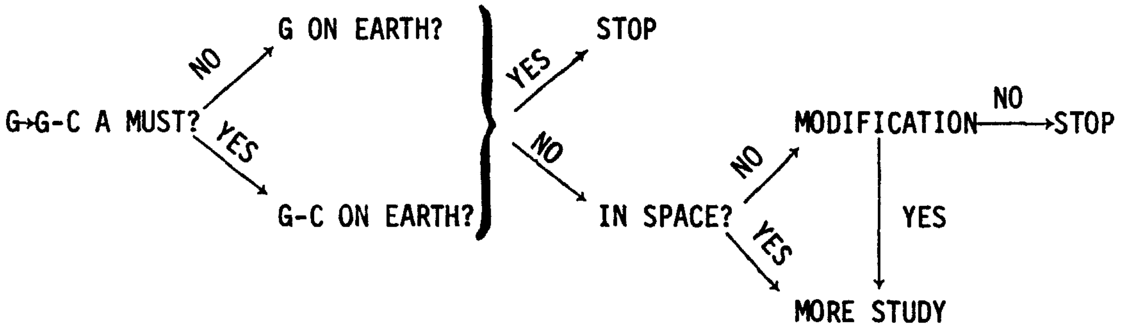

where G = Glass, G-C = Glass-Ceramics

2. Experimental study on glass formation

2.1. Selection of composition

The binary system of B_2O_3-Fe_2O_3 can be classified as shown below based upon B (boron) being 3-fold and Fe (iron) 6-fold coordination. The derivation of such a classification is shown in Appendix 1.

No. Corners Shared	Oxygen Distribution Per Boron Triangle		Fe/B	Structure Type	Formulas	Mole % B_2O_3
	Non-bridging	Bridging Oxygen				
3	0	3	0	Sheet or Framework	B_2O_3	100
2	1	2	0.2	Chain	FeB_5O_9 or $Fe_2O_3 \cdot 5B_2O_3$	83.3
1	2	1	0.5	Double Triangle	$Fe_2B_4O_9$ or $Fe_2O_3 \cdot 2B_2O_3$	66.7
0	3	0	1.0	Indep. Triangle	$FeBO_3$ or $Fe_2O_3 \cdot B_2O_3$	50

The glass formation usually improves with the number of corners shared between the basic glass-forming units such as Si-tetrahedron in silicate glass or B-triangle in borate glass. To put it in another way, the difficulties involved in preparing say the borate glass on earth usually increases with the ratio of Fe (modifying ion) over B (network forming ion), from sheet or framework (B_2O_3), to chain ($Fe_2O_3 \cdot 5B_2O_3$), to double triangle ($Fe_2O_3 \cdot 2B_2O_3$), and finally to independent triangle ($Fe_2O_3 \cdot B_2O_3$ or $FeBO_3$). The iron borate glasses so far achieved on earth usually lie somewhere between sheet and chain but much closer to the sheet structures. The chain structure such as $Fe_2O_3 \cdot 5B_2O_3$ probably represents the limit for glass formation on earth since each B-triangle possesses two bridging oxygen ions by which it can link to adjacent triangle so that rings or long chains of these triangle groups can occur. The formation of a long chain or a large ring is essential for a glass formation, because such formation of chain or ring will generate during cooling sufficiently high viscosities which will in turn lead to the glass formation. It appears that $Fe_2O_3 \cdot 5B_2O_3$ (83.3 mole % B_2O_3) of the chain structure or some composition close to it would be the most promising composition for space processing based upon the following two reasons:

(a) Likely to form glass in space

$Fe_2O_3 \cdot 5B_2O_3$ has a chain structure which as mentioned earlier usually represents the compositional limit that a material may form glass but with great difficulty on earth. Since the heterogeneous nucleation is eliminated or greatly reduced under space conditions, the prospect of forming a glass for the chain structure is likely to improve in space.

(b) Likely to have sufficient amount of $FeBO_3$ phase

Based upon the following comparison[6] with the properties of YIG, the current material used for the magneto-optic devices, amount of $FeBO_3$ phase that can be crystallized out of the composition of $Fe_2O_3 \cdot 5B_2O_3$ seems to be sufficient and adequate for the magneto-optic application.

	F (deg/cm)	α (cm^{-1})	2F/α (deg)	T (°K)	λ (mμ)
YIG	2400	1500	3.2	300	555
$FeBO_3$ (50B)	2300	40	115	300	525
$Fe_2O_3 \cdot 5B_2O_3$	1039*	40	52*	300	525

where F = Faraday rotation, α = Absorption minimum in visible, T = Temperature, and λ = wavelength

*An estimated value based on the content of $FeBO_3$ or Fe_2O_3 in 83.3B which has 45.16 wt.% Fe_2O_3 of that in 50B.

2.2. Selection of raw materials

Two types of raw materials, namely, MOD and batch oxide were used for this study. They were summarized and also described in detail separately as follows.

Raw Material	Nature	Phase Assemblage		Remarks
		Before	After Heat Treatment	
Batch Oxide	Mechanical mixture of B_2O_3 and Fe_2O_3 by ball milling	Mixture of B_2O_3 and Fe_2O_3 phases	$FeBO_3$ phase	Free B_2O_3 is very hygroscopic
MOD**	B_2O_3 and Fe_2O_3 combined by chemical reaction	Amorphous	Fe_3BO_6 or $FeBO_3$* phases	

**MOD: Raw material prepared by the Metal-Organic-Derived (MOD) method.

*$FeBO_3$ could be produced if seeded by $FeBO_3$ phase.

(a) Batch oxide

A batch oxide is prepared by mixing the right ratio of the component oxides of B_2O_3 and Fe_2O_3 and then by ball milling the mixture to insure homogeneity. The ball milling operation is necessary in view of the tremendous difference in melting point between B_2O_3 and Fe_2O_3 (460 vs. 1565°C). A comparison between the component oxides such as Fe_2O_3 and B_2O_3 is listed in Table 3. The reagent grade is used for both B_2O_3 and Fe_2O_3 to improve the quality. However, some contamination such as trace Al_2O_3 was detected after the ball milling operation.

(b) MOD

The batch material is prepared by the Metal-Organic-Derived (MOD) method. Extremely pure materials (electronic grade) can be obtained by this approach. The following example of preparing $B_2O_3 \cdot Fe_2O_3$ (50 mole % B_2O_3 or 50B) is used to illustrate the MOD approach.

$$2Fe(NO_3)_3 \cdot 9H_2O + 2B(OH)_3 \xrightarrow{\Delta} Fe_2O_3 \cdot B_2O_3 \downarrow + 6HNO_3 \uparrow + 18H_2O \uparrow$$

$Fe(NO_3)_3 \cdot 9H_2O$ (m.p. 50°C) were reacted with equal number of moles of $B(OH)_3$ at 120°C. The temperature was then raised to 180-200°C to solidify the product of $B_2O_3 \cdot Fe_2O_3$. Finally, the temperature was increased to 400°C in order to drive off the unwanted HNO_3 and water. The MOD differ from batch oxide in the following ways.

(1) The MOD materials were amorphous, while batch oxide were crystalline as confirmed by x-ray diffraction.

(2) Upon heat treatment, the MOD batch usually produced Fe_3BO_6 phase, but may produce $FeBO_3$ phase only when seeded by $FeBO_3$ phase, while batch oxide will usually produce $FeBO_3$ phase.

(3) B_2O_3 in batch oxide is hygroscopic since it exists as a free form, while B_2O_3 in MOD batch is not hygroscopic, because it is chemically combined with Fe_2O_3. In order to reduce the loss of the free B_2O_3 during melting, the batch oxide is often crystallized into $FeBO_3$ phase before making a melt.

2.3. A summary of melting conditions and melts prepared

(A) Melting conditions

The range of conditions tried is indicated as follows:

Temperature, °C: 1275-1575

Time, hr.: 2-7

Number of stirring: 0-3

Environment: air or pure oxygen at one atmosphere

(B) Quenching method

The melts were often cast by splat cooling into plate forms, sometimes by air cooling into disc forms, and occasionally by water quenching the whole crucible.

(C) Identification of melts

All the batch materials used for preparing melts were identified by a code system which may contain as many as four parts, e.g., the four parts in 83B-M-1/2Pb-3 are explained below: (1) 83B, B_2O_3 mole % = 83 excluding flux; (2) M, batch material prepared by MOD approach; (3) 1/2 Pb, half of Pb used as flux, the full amount = $0.9PbF_2$ + 0.2PbO; (4) 3, third time such batch was prepared. More examples are listed as follows:

Identification Code	B_2O_3 Mole %	Batch Material	Flux	Order of Batch Preparation	Remarks
50B-5	50	batch oxide	--	5th	M, batch by MOD, otherwise batch by batch oxide
50B-M-2	50	MOD	--	2nd	
83B-Pb/2-1	83	batch oxide	Pb/2	1st	
83B-M-Bi/2-2	83	MOD	Bi/2*	2nd	

*Full Bi = $1Bi_2O_3$

(D) Summary of melts prepared

All the melts prepared are summarized in the increasing order of molar content of B_2O_3 (B_2O_3 mole %) and listed in Table 4. Three types of materials were often obtained from a melt; they are described as follows: (a) Plates by splat cooling. The number following the plate indicates the order of plate cast, e.g., plate 1 = 1st splat plate cast. The letter (E) attached to a plate number indicates the edge of a plate. Without such an attachment, a plate analysis usually refers to that of a central plate part. (b) Discs by air cooling and (c) black materials which are parts of the melt left at the bottom of crucibles and have black appearance.

2.4. Characterization of melts

All the prepared melts were usually analyzed for the iron content by x-ray florescent or wet chemical techniques and for the phase assemblage by x-ray diffraction. In general, the iron content in a melt increases continuously from the top to the bottom part, as shown in Table 4. As for the phase assemblage of the melts, which are shown in Tables 5 and 6 and Figures 1 and 2, three types of iron phases were found; namely, (a) $Fe_2^{3+}O_3$ including both α- and γ-Fe_2O_3, (b) Fe^{2+}-compounds, which included three types of compounds and they were often found in the following decreasing order of concentration:

$$Fe^{2+}O \cdot B_2O_3,\ Fe_2^{2+}Fe^{3+}BO_5,\ Fe^{2+}O \cdot 2B_2O_3$$

and (c) $Fe_3^{3+}BO_6$, a high temperature form of iron borate. The relative amount of the three types of phases apparently change with melting temperature as shown below:

For 80-50B	Splat Plate (Top Melt)	Black Material (Bottom Melt)
Fe_2O_3 wt.%	3-75	50-84
Phase Assemblage	Low Fe-content (≤35.4%)	--
1300°C	B_2O_3	--
1400°C	B_2O_3	--
1575°C	B_2O_3	--
	High Fe-content (≥37.5%)	All black material
1300°C	Fe_2O_3, Fe^{2+} phases, Fe_3BO_6	Fe_2O_3, Fe^{2+} phases, Fe_3BO_6
1400°C	Fe^{2+} phases, Fe_2O_3, Fe_3BO_6	Fe^{2+} phases, Fe_2O_3, Fe_3BO_6
1575°C	Fe^{2+} phases, Fe_3BO_6, Fe_2O_3	Fe^{2+} phases, Fe_3BO_6, Fe_2O_3

It was noted that a splat plate with iron content as high as 35.4 wt.% Fe_2O_3 can be made amorphous, i.e., no iron phase except B_2O_3. The iron content in this splat plate (35.4% Fe_2O_3) is more than that in 83B (31.5% Fe_2O_3), and almost approaches that in 80B (36.5% Fe_2O_3). Although the amorphous splat plate of such high iron content was made only once, this observation seems to indicate that the predicted optimum composition of 83B will likely form glass under space conditions which will maintain a constant iron composition for all the melts by suppressing the iron segregation.

2.5. Problems during melting

(A) Phase separation into iron rich and poor layers

The greatest problem involved with the preparation of an iron borate melt is the iron segregation during melting. The top melt (splat plates) often contains less iron while the bottom melt (black material) more iron, apparently due to the density difference. Because of the higher iron content, the black material was anticipated and later confirmed to have a higher melting point by DTA (Differential Thermal Analysis) technique than that of the batch material used for melting, as shown below.

Composition	Fe_2O_3 wt.%		m.p. by DTA	
	Black Material (Analyzed)	Batch Material (Target)	Black Material	Batch Material
50B-2	70.6	69.64	1237	1203
70B-2	66.9	49.57	1237	1011
80B-2	63.4	36.45	1225	999

The black material usually has a fairly constant iron content which is almost independent of that of the starting batch material. This may be the reason why all the compositions from 50B through 80B has a fairly similar melting temperature of 1275-1300°C. However, the iron content of a splat plate often increases with the order of cast. In addition, the iron content of a splat plate depends upon the amount and the angle of pouring melt from crucible and there was often compositional (iron) variation within the same plate particularly between edge and center, as shown below. This makes it difficult to duplicate the same melt casts.

	Fe_2O_3 wt.%					
	Target		Plate 1	2	3	Black Material
60B-2	60.46	Central		24.5	46.2	78.0
		Edge			7.0	
70B-4	49.57	Central	33.3		59.4	78.4
		Edge			14.5	
80B-4	36.45	Central	5.5	12.4	42.4	80.1

It was found that there is little or no phase separation at compositions 50B and 55B. However, phase separation occurs in composition 60B and in those of lower iron content. The following problems have been created by the phase separation:

(1) A melt cast often has a fluctuating iron content which is almost independent of starting batch composition and is thus difficult to duplicate.

(2) A splat plate usually contains much less iron and will likely undergo partial melting during heat treatment.

(3) Because of these difficulties mentioned above, it is very difficult to evaluate on earth: (a) whether there is a need of nucleants

and (b) how to determine the optimum nucleation and crystallization conditions during the preparation of the glass-ceramic in space.

(B) Iron reduction

Iron valence will reduce from 3 to 2 at the melting temperature and the formation of Fe^{2+} tends to make the glass nontransparent (black) and nonuniform. Although all the Fe^{2+} can be later oxidized back to Fe^{3+} at a lower temperature during the heat treatment (crystallization cycle), the formation of Fe^{2+} during melting is detrimental to the formation of a transparent glass. Thus, effort should be made to eliminate or greatly lower the iron reduction.

The conversion of Fe^{3+} into Fe^{2+} during melting is chiefly a function of the melting temperature and the partial pressure of oxygen. Lower temperature and higher oxygen content tend to suppress the formation of Fe^{2+}. A check into the conversion thermodynamics[7] indicated that temperature was the major while oxygen the minor controlling factor. It appears that the following relationship between temperature and % iron reduction holds.

T, °C	% Iron Reduction
1316	30
1275	14
1200	0.6

According to an estimation, melting in pure oxygen (100%) instead of air (21% oxygen) may increase the temperature tolerance of about 75°C for the same iron reduction rate. In other words, melting in oxygen furnaces at 1275°C will likely have the same iron reduction rate as that in air furnace at 1200°C (<1%). In addition to temperature and oxygen, other controlling factors of minor importance include the melting time and composition. Time is needed to reach equilibrium between Fe^{3+} and Fe^{2+}, and the lower the iron content, the higher the iron reduction becomes. All the data on iron reduction are summarized and listed in Table 7.

2.6. Reduction of phase separation

(A) MOD batch oxide

two different types of batch materials; namely, MOD and batch oxide were used to prepare the melt. Neither of them can eliminate or reduce the phase separation. Both of them behave pretty much the same with regard to melting losses, iron content in splat plates, and phase formations. The only differences between the two batch materials are: (a) MOD is much purer than batch oxide, and (b) batch oxide will have higher melting loss if it is not crystallized into $FeBO_3$ before making the melt.

(B) Optimization of melting conditions

The melting conditions such as temperature, time, and number of stirring were purposely changed in order to try to reduce the phase separation. This attempt was also found to be not very fruitful. Both the melting time and the number of stirring have very little or no effect on phase separation. Only melting temperature has some effect. A higher temperature such as 1575°C can slightly reduce the phase separation, as evidenced by the smaller difference in iron content between the bottom and top melts as shown below.

T,°C (80B)	t,hr.	No. Stir	Fe_2O_3 wt.%				Difference in Fe_2O_3 wt.%	
			Target	Black Mat'l (b)	Plate 1 (1)	2 (2)	b-1	b-2
1275	3	1	36.45	74.4		6.5		67.9
1275	3	1	36.45	76.1	2.9		73.2	
1300	3	1	36.45	71.1		2.8		68.3
1575	3	1	36.45	49.9	12.7		37.2	

However, a higher temperature, such as 1575°C will also produce more iron reduction which has been shown to be undesirable.

(C) Use of flux

Utilization of a flux, Bi_2O_3 or PbF_2 + PbO, was found to be successful not only in eliminating the phase separation but also in minimizing the iron reduction problem. The compositions with flux were the same ones used in the literature[4,8] for growing single crystals of $FeBO_3$; namely,

$Fe_2O_3 \cdot 5B_2O_3 \cdot Bi_2O_3$, and $Fe_2O_3 \cdot 5B_2O_3 \cdot 0.9PbF_2 \cdot 0.2PbO$

A uniform and fluid melt was obtained for both compositions at 1200°C. All splat plates produced from the two melts were found to be amorphous but opaque. In addition, it was anticipated that the iron valence reduction would be less than 1%, since the two melts were prepared at the relatively low temperature of 1200°C. However, the disadvantage of using flux is that the amount of $FeBO_3$ phase produced during the crystallization amounts only to about 1/3 of the amount without flux for the case of Bi as flux and to about 1/2 for Pb as flux, as shown in Figures 3 and 4. In order to increase the $FeBO_3$ phase, the amount of flux has to decrease. But, the reduction of flux will increase the melting temperature and the chance of phase separation. When only half of the flux was used, the melting temperature increased from 1200 to 1275°C, but the phase separation still occurred for both Bi and Pb. Phase separation was not eliminated until 3/4 Pb was used while the melting temperature was 1250°C. The data on flux is listed in Tables 4 and 8. Overall, Pb was found to be a better flux than Bi, because it renders the iron borate melt more fluid and less subject to phase separation. Finally, the optimum amount of flux will be determined by consideration of the melting temperature and the output of $FeBO_3$ phase, in addition to the elimination of phase separation.

2.7. Minimization of iron reduction

(A) Determination of minimum melting temperature

Since the iron reduction (the conversion of Fe^{3+} to Fe^{2+}) is mainly controlled by the melting temperature, the most effective way of lowering the iron reduction is to melt the iron borate material at the lowest possible melting temperature, which is determined as follows. The material is melted at the test temperature for at least one hour. Take out the crucible from the furnace at the temperature and then quickly stir with a Pt-rod or empty the whole crucible. If no solid or scum is left at the bottom or the wall, all material must go into the solution and the test temperature is the correct melting temperature. The minimum melting temperature for 80B composition appears to be 1275°C and at this temperature a 14% reduction from Fe^{3+} to Fe^{2+} was observed.

(B) Use of oxygen furnace

According to an estimation based upon conversion thermodynamics,[7] melting iron borate in an oxygen furnace (100% oxygen) instead of air (21% oxygen) may increase the temperature tolerance by 75°C for the same conversion rate, or could lower the iron reduction to less than 1% as shown below. If iron borate is melted at 1275°C in an oxygen furnace, the reduction rate may correspond to that of melting at 1200°C in air which has an iron reduction rate less than 1%. Thus, it is anticipated that by using oxygen for air, the iron reduction can be lowered to less than 1%. The effect of oxygen was tested by melting a 80B-5 at 1300°C for 3 hr. in an oxygen furnace operated at 1 atmosphere of oxygen. The data reported here should be regarded as tentative, because only one run was made and furthermore a leakage was developed in the furnace. The iron reduction was found to be 20.3% for the top melt and 25.5% for the bottom melt, or 22.9% for the average melt as also shown in Table 7. The average iron reduction of 22.9% in oxygen is almost identical to the value of 23% estimated by extrapolation of the available iron reduction data in air as shown below.

T, °C	Environment	% Iron Reduction
1316	Air	30
1275	Air	14
1200	Air	0.6
1300	Air	23 (extrapolation)
1300	Oxygen	20.3 (top melt)
1300	Oxygen	25.5 (bottom melt)
1300	Oxygen	22.9 (average melt)

Thus, it appears that oxygen has almost no effect on controlling the iron reduction. However, a confirmation will be needed before any definite conclusion can be drawn, especially in view of the fact that we have encountered lots of difficulties in using the oxygen furnace.

3. Experimental study on glass-ceramic formation

3.1. Phase assemblage in binary system of Fe_2O_3-B_2O_3

Ordinarily, there are two major phases existing in the binary system of Fe_2O_3-B_2O_3; namely, low temperature form ($FeBO_3$) and the high temperature form (Fe_3BO_6). These two phases are detailed in Table 9. In addition, Fe^{2+} phases of iron borates will be formed if the temperature is over 1200°C. The iron borate phase diagrams reported in the literature[5] were only limited to those temperatures lower than 1200°C. In other words, no Fe^{2+} phase was reported in the phase diagram. All the iron borate phases are summarized and discussed below. Their x-ray diffraction patterns were identified in Table 10 and illustrated in Figures 5 and 6.

Type of Material	Temperature Change		Iron Content*	Phase assemblage
	Nature	Range		
Batch	Crystallization	RT → <800°C	≤50B	$FeBO_3$
			>50B	Fe_3BO_6, Fe_2O_3, $FeBO_3$
Melt	Quenching	>1200°C → RT	≤50B	Fe_2O_3, Fe^{2+} phases, Fe_3BO_6

Note: RT = Room Temperature,

* The iron content of 50B being 69.64 wt.% Fe_2O_3, ≤50B being less than and equal to that, while >50B being greater than that.

(A) $FeBO_3$ phase (low temperature form)

The $FeBO_3$ phase has many unique properties and is thus the one we are after. The $FeBO_3$ phase can be formed exclusively from the batch compositions of 80B-50B at a crystallization temperature below 800°C, say 680°C. Since only the composition of 50B can form 100% $FeBO_3$ ($Fe_2O_3 \cdot B_2O_3$) phase, one wonders whether a composition like 80B or 83B ($Fe_2O_3 \cdot 5B_2O_3$, the predicted optimum composition) will form a $FeBO_3$ solid solution upon crystallization, or if a solid solution is not possible, whether it will simply form $2FeBO_3 + 4B_2O_3$. This type of information would be very useful for arriving at the proper heat treatment. Based upon the structural information, no solid solution will be formed from $FeBO_3$ because B differs from Fe not only in size but also in coordination, i.e., Fe-6(BO_3), and B-3(O). The prediction by structural information is confirmed below. Upon crystallization the 80B composition was found to produce a crystalline $FeBO_3$ phase (see Figure 7) identical in d-spacing to that of 50B composition. As might be expected, it did take a little bit longer to completely crystallize $FeBO_3$ out from 80B than from 50B; namely, 680°C-4 days vs. 680°C-3 days. However, the crystalline B_2O_3 phase was not observed during the crystallization of 80B at 680°C for 4 days.

(B) Fe_3BO_6 (high temperature form)

Fe_3BO_6 will be formed when the compositions of 50B and those of lower iron content are heat treated at temperatures over 800°C, or when the compositions of higher iron content than that in 50B are heat treated at temperatures below 980°C. Since it is easy to form Fe_3BO_6 and to have a boron of 4-fold coordination (which makes it difficult to form glass) in the region of iron content higher than that in 50B, no composition in this region is used in this study.

(C) Fe^{2+} phases

Fe^{2+} phases will form when the iron borates (Fe_2O_3-B_2O_3) are heat treated or melted at temperatures over 1200°C. The common Fe^{2+} phases are $Fe^{2+}O \cdot B_2O_3$, $Fe_2^{2+}Fe^{3+}BO_5$, and $Fe^{2+}O \cdot 2B_2O_3$ as shown in Table 10.

3.2. Necessity of glass-ceramics

As compared to other iron oxygen compounds such as spinels, garnets, and orthoferrites, only $FeBO_3$ single crystals have unique properties such as stronger magnetization and lower absorption in the visible which are attributed to its unique coordination. The Fe in $FeBO_3$ is coordinated to 6(BO_3) rather than 6(oxy.). The amorphous and the high temperature (Fe_3BO_6) phase of iron borate are expected to have little or no magnetization due to the difference in their Fe coordination. This was found to be the case as shown below:

Phase	Fe Coordination	Spontaneous Magnetization M_s, emu/gm
$FeBO_3$ (low-temperature phase)	6(BO_3)	> 1.0
Fe_3BO_6 (high-temperature phase)	6(BO_4)	0
Amorphous	random	0

Therefore, the crystalline material rather than the glass is essential to obtain the unique properties of $FeBO_3$. In view of the drawbacks associated with the earth-prepared single crystals and ceramic materials, as mentioned in Table 2, glass-ceramics become very attractive.

3.3. Problems during crystallization

(A) Partial melting

Upon heat treatment at crystallization temperature (680°C), the splat plates with less iron content will change shape, soften, or even partially melt before crystallization. Of course, this problem was originated from the phase separation which happened at the melt. This type of problem is caused not only by the low iron content but also by the uneven iron distribution over the same plate. Two 83B compositions were made up for comparison as follows: The first one, 83B(1) was made up by mixing the top and the bottom melts at the proper ratio according to the analyzed iron content in each part, while the second one, 83B(2), was prepared by using a proper batch oxide. The batch oxide was prepared by directly ball milling a proper mixture of Fe_2O_3 and B_2O_3. It was found that during the heat treatment at 680°C for 1 hr., 83B(2) underwent virtually no shape change but there was great change in shapes for 83B(1). The difference is likely caused by the uneven iron distribution. Since a mixture as uniform as that in 83B(2) can be achieved in space, this type of drawback can likely be overcome by space processing.

(B) Unwanted phases

The melt casts which were prepared on earth at 1300°C or higher temperatures and had a Fe content equal to or more than 37.5 wt.% Fe_2O_3 usually contained the following unwanted phases.

Fe_2O_3, Fe^{2+} phases, and Fe_3BO_6

Upon heat treatment at 680°C, all Fe^{2+} can be oxidized into Fe^{3+} if sufficient oxygen can be made available. Also all the crystalline phases in the melt were transformed into the $FeBO_3$ phase plus some small amounts of Fe_2O_3 and maybe B_2O_3. The 50B composition which contains the highest iron content and has no phase separation was found to have the maximum $FeBO_3$ phase. Whether the absence of a phase separation can help to boost the $FeBO_3$ phase remains to be seen. In addition, there is a possibility that all Fe^{2+} phases may be eliminated from the melts if oxygen is used to replace air during the melting.

(C) Need of nucleant

Fe_2O_3 is known to be a good nucleant. Whether there is a need of nucleant in the preparation of glass-ceramic from Fe_2O_3-B_2O_3 can be decided by checking the bulk versus the surface crystallization without the use of a nucleant. No nucleant is needed if a bulk crystallization can be achieved in a controllable fashion without the start of surface before bulk crystallization. A test of such a need becomes very difficult due to the phase separation taken place in the terrestrial preparation. The iron poor (top) melt which although can form an amorphous splat plate will often undergo partial melting during crystallization, while the iron-rich (bottom) melts are easily devitrified and have lots of unwanted phases such as Fe_2O_3, Fe_3BO_6 and maybe Fe^{2+} phases if steps were not taken to prevent their formation. However, there is still a possibility that such a test can be made on earth through the use of flux or the composition of 50B where no phase separation is observed.

3.4. Properties measurement

(A) Magnetic properties

A vibrating sample magnetometer manufactured by Princeton Applied Research Cooperation (Model 155) was used to measure the spontaneous magnetization (M_s). The findings are reported as follows.

(a) Since ferromagnetic materials such as the crystalline $FeBO_3$ phase are the only materials that can produce a strong M_s below the Curie temperature, T_c, the measurement of M_s is a good way to distinguish the crystalline $FeBO_3$ phase from all the rest of the materials involved and produced in the preparation of the iron borate glass-ceramics. The measured M_s values are summarized as below.

M_s, emu/gm		
None (0)	Weak (0.1)	Strong (≥ 1)
(1) Amorphous $FeBO_3$ (2) Crystalline Fe_3BO_6 phase (3) Melts without any crystalline iron compounds	(1) α-Fe_2O_3 (raw material) (2) Melts with Fe^{2+} iron borate phases	(1) Crystalline $FeBO_3$ phase

(b) The crystalline $FeBO_3$ phase obtained by heat treating the batch material of 50B-1 at 680°C for 5 days showed good agreement on magnetic properties with the literature data,[1,2] as indicated below:

Source	Type of Sample	M_s, emu/gm	T_c, °C
Literature	Powder	1.5	115
Literature	Single crystal	2.1	75
Our measurement	Powder	1.38	75

(c) Due to the phase separation, the top melts such as the splat plates often contain much lower iron content than the original. Thus, the glass-ceramic upon crystallization has much smaller iron borate content. On the other hand, an iron borate glass-ceramic produced without the adverse effect of phase separation, e.g., 50B on earth or all compositions processed in space can produce a M_s as large as that of the corresponding batch material properly crystallized. These are illustrated as follows:

Sample	Mole % B_2O_3	M_s, emu/gm	
		Batch + 680°C-5 days	Splat Plate + 721°C-4 days
50B-1	50	1.38	1.40
60B-1	60	1.33	1.26
70B-1	70	1.12	0.92
80B-1	80	0.81	0.08
90B-1	90	0.47	0.10

The difference in M_s from 60B through 90B is caused by the phase separation.

(d) The spontaneous magnetization (M_s) was found to be proportional to the active phase of crystalline $FeBO_3$ which was in turn roughly proportional to the Fe_2O_3 content in the starting material, as shown below.

Sample	Wt.% Fe_2O_3	Wt. Ratio Fe_2O_3	M_s, emu/gm	
			Observed Value (Batch + 680°C-5 days)	Calculated Value (Based on 1.33 for 60B)
50B-1	69.64	1.1518	1.38*	1.53
60B-1	60.46	1.0	1.33	1.33
70B-1	49.57	.8199	1.12	1.09
80B-1	36.45	.6029	0.81	0.80
90B-1	20.31	.3359	0.47	0.45

*$FeBO_3$ was not completely crystallized, some Fe_2O_3 left.

If the spontaneous magnetization (M_s) is roughly proportional to the Fe_2O_3 content, the iron content may also be estimated from the magnetometer data measured on crystallized iron borate such as the splat plate at 721°C for 4 days. This was found to be the case as shown below.

Sample	Mole % B_2O_3	Wt. % Fe_2O_3			
		Target	Wet Chemical	X-Ray Florescent	Magnetometer
50B-1	50	69.64	70.06	69.17	63.7
60B-1	60	60.46	61.02		57.3
70B-1	70	49.57			42.0
80B-1	80	36.45		4.3	4.1
90B-1	90	20.31	3.1	4.0	4.5

(B) Other measurements

(1) Infrared transmission

Based upon a structural consideration, the 50B composition is not likely to form a glass even in space. Thus, its chance to be transparent in the visible is almost nil. However, the 50B composition prepared on earth is free from phase separation, undergoes no shape change during crystallization, and can completely transform into one $FeBO_3$ phase from the crystallized melt. Although the glass-ceramic made from the 50B composition is opaque in the visible, it could have some potential use in laser applications if it is transparent in the infrared, e.g., at 1.06 μ. The following 50B composition was tested for the transparency at 1.06 μ for the potential use in laser application. A 50B-1 composition was melted at 1316°C for 7 hrs., and then its splat plate was heat treated at 721°C for 4 days. A thin section of such prepared material was checked for the transparency at 1.06 μ by a Nd-laser. Little (less than 1%) transmission at 1.06 μ was observed.

(2) Faraday rotation

The splat plate of 90B-2 melted at 1316°C and bubbled with oxygen had amber color and was translucent. The transmission in visible and infrared region (1.06 μ) were 1.4 and 43.1%, respectively. Upon crystallization at 721°C, the splat plates of 80B-1 and 90B-1 which were also prepared at 1316°C, but without the bubbling of oxygen underwent the partial melting and the re-crystallization. For these two compositions 80B-1 and 90B-1, the re-crystallized material in general had clear outer edges likely to be B_2O_3 glass, narrow red inner edge likely to be Fe_2O_3, and the deep green interior of $FeBO_3$ interspersed with numerous voids. The green interior was translucent but due to void-caused scattering the transmission in the visible was poor, e.g., the highest transmission measured on a good spot was only 34%. Due to the numerous voids, there were too much scattering. The Faraday rotation was measured but was meaningless because of the depolarization caused by the diffusely scattered light.

(3) Particle size of prepared melt

The air-quenched disc was used to measure the particle size of the two melts of 80B-1 and 90B-1 prepared at 1316°C for 7 hrs. The particle size was determined by the electron micrograph (using a fracture surface but no etching) and the associated phase assemblage by x-ray diffraction as shown below.

Type of Particle	Particle Size, μ		Phase Assemblage
	80B-1	90B-1	
Big	1.7	1.0	Crystalline B_2O_3
Small	0.2	0.2	$FeBO_3$ phase to be crystallized later
Matrix	<< 0.2	<< 0.2	Glass

Note: The wavelength of visible light ranges from 0.4 to 0.7 μ.

Although the particle size of crystalline B_2O_3 is larger than the wavelength of light (about 0.5 μ), the amount of B_2O_3 phase present is relatively small. Since the majority of the particle sizes are smaller than the wavelength of light, there is a possibility that a transparent glass may be formed if the formation of melt can be controlled and processed in space.

4. Conclusions

(1) The optimum composition suitable for space processing was estimated to be 83B, i.e., $Fe_2O_3 \cdot 5B_2O_3$ for the binary system of B_2O_3-Fe_2O_3.

(2) The glass-ceramic rather than the glass was found to be necessary for providing the unique magneto-optical properties of $FeBO_3$.

(3) The two terrestrial obstacles in the preparation of $FeBO_3$; namely, phase separation and iron reduction were identified. Different approaches were tried but so far failed to overcome these obstacles. Thus, it is reasonable to say that a transparent $FeBO_3$ glass-ceramic cannot be prepared on earth at the present time.

(4) The calculated composition is expected to form glass in space, since a splat plate with a similar iron content formed a glass on earth. However, it is extremely difficult to produce a glass of constant composition on earth due to the phase separation.

(5) Once converted into a glass in space, the calculated composition will not have any of the unwanted crystalline phases existed for the partially crystallized melt prepared on earth. Since the particle sizes of splat plates prepared on earth are smaller than the wavelength of the visible light, the prospect of obtaining a transparent glass in space from this calculated composition is good, particularly if steps can be found and taken to eliminate or greatly lower the iron reduction.

(6) Once a transparent glass is formed in space, the prospect of obtaining a transparent glass-ceramic will mainly depend upon whether a controllable crystallization can be achieved. A controllable crystallization which may be performed even on earth involves the determination of (a) a need of nucleant, and (b) time and temperature relationship for both nucleation and crystallization cycles.

5. Recommendations

(1) Continue the study to determine parameters that will minimize phase separation and iron reduction. Particularly, the effect of oxygen on iron reduction will be double-checked in order to see if the advantages predicted by thermodynamics can be realized.

(2) Study the true nature of the phase separation in terms of (a) how and when the separation starts, (b) the type of separation and (c) the possible effect of melting temperature, time, composition and rate of quenching.

(3) Determine the need of nucleants and the optimum nucleation and crystallization conditions for the terrestrial formation of $FeBO_3$ crystals. Those compositions which have no phase separation problem such as 50B or 83B with flux may be used for such a determination.

(4) Determine the limit of iron borate glass formation on earth and the range of particle sizes vs. iron content of splat plates prepared on earth.

(5) Determine the optimum raw material preparation and melting conditions, and prepare samples for test in space.

(6) Continue the assessment, both technical and economical of space processing of $FeBO_3$ glass-ceramics.

References

1. R. Wolfe, A. J. Kurtzig, and R. C. LeCraw, J. Appl. Phys., 41, 1218 (1970).
2. J. C. Joubert, T. Shirk, W. B. White and R. Roy, Mat. Res. Bull., 3 671 (1968).
3. A. J. Kurtzig, R. Wolfe, R. C. LeCraw, and J. W. Nielson, Appl. Phys. Letters, 14, 350 (1969).
4. R. C. LeCraw, R. Wolfe, and J. W. Nielson, Appl. Phys. Letters, 14, 352 (1969).
5. H. Makram, L. Touron and J. Loriers, J. Crystal Growth 13/14, 585 (1972).
6. R. J. Pressley, Handbook of Laser (Chapter 16, "Magneto-optic Materials," by D. Chen, C. R. C. Press Inc., 460, (1971)).
7. R. A. Swalin, Thermodynamics of Solids (John Wiley and Sons Inc., 84, (1962)).
8. I. Bernal, C. W. Stuck, and J. G. White, Acta Cryst. 16, 849 (1963).

Table 1

Properties of $FeBO_3$ Single Crystals

	$FeBO_3$ Single Crystals
Curie temperature, T_c	348°K or 75°C
Spontaneous moment, $4\pi M_s$	115G
Saturation or spont. magnetization M_s	9.15 gauss/cm^3
	2.1 emu/gm
	4.5×10^{-2} μ_B/mole
Absorption band edge $\alpha = 1000\ cm^{-1}$	4500 Å
Absorption minimum in green	39 cm^{-1} at 5250 Å
Faraday rotation in green	2300°/cm at 5250 Å
Faraday rotation/absorption (green)	14°/dB
Indices of refraction (green)	$\approx$ 2.1
Density	4.3 g/cm^3
Birefringent phase retardation	-4×10^5 deg/cm at 5250 Å

Table 2

A Comparison of Different Forms of $FeBO_3$

	$FeBO_3$		
	Single Crystals	Ceramic	Glass-Ceramic
Availability	Now	Now	Future
Birefringence	Yes	No	No
Size control	Poor	Poor	Good
Transparency	Good	Poor	Good
Smooth surface	Likely	Difficult	Likely
Cost	High	Low	Low
Suitability for magneto-optic application	Poor	Poor	Excellent

Note: (1) Birefringence not only greatly interfers with the Faraday roation but also causes a phase retardation of 4.2×10^5 deg/cm at $\lambda = 5250$ Å.

(2) A poor size control such as a typical single crystal can only grow to a size of a few mils thick and up to a few mm across usually means that the desirable shape cannot be prepared or sometimes can only be prepared with great difficulty and expense.

(3) Transparency is one of the essential properties in $FeBO_3$. Without the transparency, $FeBO_3$ will be of little value in the magneto-optic application.

Table 3

Raw Material Used in Preparation of Iron Borate Melt

	Molecular Wt.	Density y/cm^3	m.p. °C	Color	Solubility Cold H_2O	Solubility Hot H_2O
Fe_2O_3 (Hematite)	159.69	5.24	1565	red brown to black	i	i
B_2O_3	69.62	2.46	460	white or colorless	sl.s.	s
Bi_2O_3	495.96	8.55	860	light white yellow	i	i
PbF_2	245.19	8.24	855	collorless	sl.s.	
PbO	223.19	9.53	888	yellow	sl.s.	

Note: i = insoluble, S = soluble, sl. = slightly

Table 4 A Summary of Melts Prepared

Ident. Code	Batch Heat Treat.	Melting Condition			Loss %	Fe$_2$O$_3$ wt.%			
		T,°C	t,Hr.	No. Stir		Target	Raw Mat'l	Type Melt	% Fe$_2$O$_3$
50B-1	--	1316	7	1	5.2	69.64		disc	70.06
								plate	70.42
50B-2	680°C-4d	1300	5.9	2	3.9	69.64		disc	50.9
								plate	57.4
								black mat'l	70.6
50B-3	680°C-4d	1300	3	1		69.64	71.2	plate 1	65.9
								black mat'l	78.9
50B-3	680°C-3d	1575	3	1	4.7	69.64	71.2	plate 1	75.0
								black mat'l	72.1
50B-M-1	680°C-25hr	1300	5.9	2	4.9	69.64		disc	58.6
								plate	68.5
								black mat'l	69.6
								red peeling	11.7
55B-1	680°C-4d	1300	3	1	5.3	65.24	65.1	plate 1	67.1
								black mat'l	75.9
60B-1	--	1316	7	1	8.6	60.46		disc	64.73
								plate	61.02
60B-2	680°C-4d	1285	2	2	1.8	60.46	61.0	plate 2	24.5
								plate 3	46.2
								plate 3(E)	7.0
								black mat'l	78.0
60B-M-1	680°C-1d	1285	2	2	2.1	60.46	63.2	plate 1	5.4
								plate 3	37.8
								black mat'l	84.4
70B-2	680°C-4d	1300	6	2	3.5	49.57		disc	27.2
								plate	35.4
								black mat'l	66.9
70B-4	650°C-3d	1275	3	1	4.3	49.57	49.2	plate 2	11.0
								black mat'l	77.6
70B-4	650°C-3d	1300	6	2	20.8*	49.57	49.2	plate 1	33.3
								plate 3	59.4
								plate 3(E)	14.5
								black mat'l	78.4
70B-M-1	680°C-25hr	1300	6	2	2.0	49.57		disc	33.7
								plate	37.5
								black mat'l	63.3
70B-M-2	650°C-3d	1275	3	1	2.5	49.57	47.0	plate 1	3.1
								black mat'l	77.43
70B-M-2	650°C-3d	1300	6	2	29.8*	49.57	47.0	plate 1	4.6
								plate 3	20.9
								black mat'l	78.6
80B-1	--	1316	7	1	32*	36.45		plate	4.26
80B-2	680°C-4d	1300	5.7	3	4.8	36.45	33.0	disc	28.7
								plate	10.6
								black mat'l	63.4
80B-2	--	1300	2	1	3.7	36.45	33.0	top	3.7
								bottom	61.9
80B-2	--	1400	2	1	3.5	36.45	33.0	top	5.6
								bottom	58.9
80B-5	600°C-4d	1300	3	oxy.	8.9	36.45		top	2.3
								bottom	67.8

Table 4 A Summary of Melts Prepared

Ident. Code	Batch Heat Treat.	Melting Condition			Loss %	Fe_2O_3 wt.%			
		T,°C	t,Hr.	No. Stir		Target	Raw Mat'l	Type Melt	% Fe_2O_3
80B-3	--	1300	6	2	4.3	36.45	35.0	plate 2 black mat'l	2.8 70.5
80B-3	--	1300	6	1	24.1*	36.45	35.0	plate 2 black mat'l	2.9 70.1
80B-3	--	1300	3	0	10.3	36.45	35.0	plate 1 plate 2 plate 3 black mat'l	3.0 2.8 3.4 71.5
80B-3	--	1300	3	1	21.4*	36.45	35.0	plate 2 black mat'l	2.8 71.1
80B-4	650°C-3d	1275	3	1	1.3	36.45	38.1	plate 2 black mat'l	6.5 74.4
80B-4	650°C-3d	1300	6	2	2.4	36.45	38.1	plate 1 plate 2 plate 3 black mat'l	5.5 12.4 42.4 80.1
80B-4	680°C-3d	1575	3	1	3.6	36.45	38.1	plate 1 black mat'l	12.7 49.9
80B-M-1	650°C-3d	1275	3	1	1.2	36.45	36.6	plate 1 black mat'l	2.9 76.13
80B-M-1	650°C-3d	1300	6	2	1.5	36.45	36.6	plate 2 black mat'l	4.8 77.8
82B-M-1	680°C-25hr	1300	5.7	2	1.4	33.49		disc plate black mat'l	31.9 39.9 63.3
83B-Bi-1	--	1200	4	1	5.6	16.4	14.2	plate 1 plate 5	15.2 16.1
83B-1/2Bi-1	--	1275	3	1	1.0	21.32		plate 1 plate 3	16.1 24.6
83B-Pb-1	--	1200	4	1	8.3	20.4	19.6	plate 1 plate 5	20.8 21.0
83B-1/2Pb-1	--	1275	4	1	5.4	24.75		plate 1 plate 5	5.8 43.0
83B-3/4Pb-1	--	1250	1.5	--	6.0	22.37		plate 1 bottom mat'l	21.4 22.2
83B-7/8Pb-1	--	1225	3	1	6.5	21.35		plate 1 plate 2	20.1 19.9
90B-1	--	1316	7	1	22.7*	20.31		disc plate black mat'l	3.33 3.13 32.0

*holes in crucibles

Table 5 Phase Assemblages for Splat Plate (Top Material) of Melts

Temp.-Time °C-Hr.	Composition Ident.	Fe_2O_3 Wt.%		Phase Assemblage (arranged in order of decreasing intensity)
		T	A	
1300-2	80B-2	36.45	3.7	B_2O_3, $FeO \cdot B_2O_3$
1300-5.7	80B-2	36.45	10.6	B_2O_3
1300-5.7	82B-M-1	33.49	39.9	Fe_2O_3, B_2O_3, $FeO \cdot B_2O_3$, Fe_2FeBO_5, Fe_3BO_6, $FeO \cdot 2B_2O_3$
1300-5.9	50B-2	69.64	57.4	Fe_2O_3, $FeO \cdot B_2O_3$, Fe_2FeBO_5, Fe_3BO_6, $FeO \cdot 2B_2O_3$
1300-5.9	50B-M-1	69.64	68.5	Fe_2O_3, $FeO \cdot B_2O_3$, Fe_2FeBO_5, $FeO \cdot 2B_2O_3$, Fe_3BO_6
1300-6	70B-2	49.57	35.4	B_2O_3
1300-6	70B-M-1	49.57	37.5	B_2O_3, Fe_2O_3, $FeO \cdot B_2O_3$, Fe_2FeBO_5
1316-7	50B-1	69.64	70.42	Fe_2FeBO_5, Fe_2O_3, $FeO \cdot 2B_2O_3$, $FeO \cdot B_2O_3$, Fe_3BO_6
1316-7	60B-1	60.46	61.02	Fe_2O_3, $FeO \cdot B_2O_3$, Fe_2FeBO_5, B_2O_3, $FeO \cdot 2B_2O_3$, Fe_3BO_6
1316-7	80B-1	36.45	4.3	B_2O_3
1316-7	90B-1	20.31	3.13	B_2O_3
1400-2	80B-2	36.45	5.6	B_2O_3
1575-3	50B-3	69.64	75.0	$FeO \cdot 2B_2O_3$, Fe_2FeBO_5, Fe_3BO_6, $FeO \cdot B_2O_3$, Fe_2O_3
1575-3	80B-4	36.45	12.7	only amorphous

Note: All the phases assemblages reported here are for the first splat plates.

Table 6 Phase Assemblages for Black (Bottom) Material of Melts

Temp.-Time °C-Hr.	Composition Ident.	Fe_2O_3 Wt.%		Phase Assemblage (arranged in order of decreasing intensity)
		T	A	
1300-2	80B-2	36.45	61.9	Fe_2O_3, Fe_2FeBO_5, $FeO\cdot B_2O_3$, $FeO\cdot 2B_2O_3$, Fe_3BO_6
1300-5.7	80B-2	36.45	63.4	Fe_2O_3, $FeO\cdot B_2O_3$, Fe_2FeBO_5, $FeO\cdot 2B_2O_3$, Fe_3BO_6
1300-5.7	82B-M-1	33.49	63.3	Fe_2O_3, $FeO\cdot B_2O_3$, $FeO\cdot 2B_2O_3$, Fe_2FeBO_5, Fe_3BO_6
1300-5.9	50B-2	69.64	70.6	Fe_2O_3, $FeO\cdot B_2O_3$, Fe_2FeBO_5, $FeO\cdot 2B_2O_3$, Fe_3BO_6
1300-5.9	50B-M-1	69.64	69.6	Fe_2O_3, $FeO\cdot B_2O_3$, Fe_2FeBO_5, $FeO\cdot 2B_2O_3$, Fe_3BO_6
1300-6	70B-2	49.57	66.9	Fe_2O_3, $FeO\cdot B_2O_3$, Fe_2FeBO_5, Fe_3BO_6, $FeO\cdot 2B_2O_3$
1300-6	70B-M-1	49.57	63.3	Fe_2O_3, $FeO\cdot B_2O_3$, Fe_2FeBO_5, $FeO\cdot 2B_2O_3$, Fe_3BO_6
1400-2	80B-2	36.45	58.9	$FeO\cdot B_2O_3$, Fe_2FeBO_5, $FeO\cdot 2B_2O_3$, Fe_2O_3, Fe_3BO_6
1575-3	50B-3	69.64	72.1	Fe_2FeBO_5, $FeO\cdot B_2O_3$, $FeO\cdot 2B_2O_3$, Fe_3BO_6, Fe_2O_3
1575-3	80B-4	36.45	49.9	$FeO\cdot B_2O_3$, Fe_3BO_6, $FeO\cdot 2B_2O_3$, Fe_2FeBO_5

Table 7

A Summary of Iron Reduction vs. Temperature, Time, and Composition

			Melting Condition		Fe_2O_3 Wt.%		% Conversion
Sample	Raw Material	Type of Melt	Temp., °C	Time, Hr.	Analyzed	Target	$Fe^{3+} \rightarrow Fe^{2+}$
50B	batch	disc	1316	7	70.06	69.64	30.1
50B	batch	plate	1316	7	70.42	69.64	29.9
80B	batch	black mat'l	1300	2	71.79	36.45	19.03
90B	batch	disc	1316	7	3.33	20.31	29.4
90B	batch	plate	1316	7	3.13	20.31	28.1
80B	batch	top	1300	3	2.32	36.45	20.3
80B	batch	bottom	1300	3	67.83	36.45	25.5
70B	MOD	black mat'l	1275	3	77.43	49.57	13.82
70B	batch	black mat'l	1275	3	77.58	49.57	14.77
80B	MOD	black mat'l	1275	3	76.13	36.45	13.35
80B	batch	black mat'l	1275	3	74.40	36.45	17.20
50B	batch	all	1200	24	72.04	69.64	0.56
50B	batch	all	1200	2	68.90	69.64	0.32
80B	batch	all	1200	24	39.73	36.45	0.96
80B	batch	all	1200	2	37.29	36.45	0.64

Table 8

A Summary of Flux Compositions

		Fe_2O_3 Wt.%					
Sample	T,°C	Target	Batch	1st Plate	Last Plate	Phase Separation	Remarks
83B-Bi-1	1200	16.4	14.2	15.2	16.1	No	83B-Bi: $Fe_2O_3 \cdot 5B_2O_3 \cdot Bi_2O_3$
83B-1/2Bi-1	1275	21.32		16.1	24.6	Yes	
83B-Pb-1	1200	20.4	19.6	20.8	21.0	No	83B-Pb: $Fe_2O_3 \cdot 5B_2O_3 \cdot 0.9PbF_2 \cdot 0.2PbO$
83B-1/2Pb-1	1275	24.75		5.8	43.0	Yes	
83B-3/4Pb-1	1250	22.37		21.42	22.0	No	
83B-7/8Pb-1	1225	21.35		20.05	19.94	No	

Table 9

Phase Assemblage in B_2O_3-Fe_2O_3

	$FeBO_3$	Fe_3BO_6
Phase	low temp. form	high temp. form
Decomposition temp. (°C)	900	980
Structure	calcite	norbergite
Space group	$R\bar{3}C$	Pnma
Lattice constants		
a (Å)	4.613	10.05
b (Å)		8.55
c (Å)	14.42	4.47
Coordination		
B	3	4
Fe	6	6
Oxy.	2Fe+1B	3Fe+2/3B or 1/3(3Fe)+2/3(3Fe+1B)

Table 10 Identification of Common Phases

(d-spacing/2θ (cu) in order of decreasing intensity

$FeBO_3$	Fe_2O_3 Hematite	Fe_3BO_6	$FeO\cdot B_2O_3$	$FeO\cdot 2B_2O_3$	Fe_2FeBO_5	B_2O_3	$PbO\cdot 2B_2O_3$	$Bi_2O_3\cdot Fe_2O_3$	$PbO\cdot 2Fe_2O_3$
2.683/33.36 (100)	2.69/33.28 (100)	2.96/30.16 (100)	4.48/19.8 (100)	5.5/16.08 (100)	2.58/34.74 (100)	3.21/27.78 (100)	2.673/33.5 (100)	3.95/22.48 (100)	2.64/33.94 (100)
3.50/25.4 (60)	1.69/54.24 (60)	3.69/24.1 (60)	2.64/33.92 (100)	4.2/21.12 (90)	5.16/17.16 (50)	6.08/14.56 (35)	3.952/22.48 (80)	2.811/31.80 (95)	2.81/21.82 (60)
2.084/43.38 (30)	2.51/35.74 (50)	2.56/35.02 (60)	2.83/31.58 (70)	3.49/25.5 (60)		3.80/23.4 (25)	5.423/16.34 (75)	2.783/32.14 (80)	2.96/30.18 (40)
1.668/55 (30)	1.838/49.6 (40)	2.48/36.2 (30)	2.58/34.74 (50)	2.24/40.22 (60)			4.122/21.54 (75)	1.614/57.0 (55)	
2.31/38.96 (18)	2.201/40.96 (30)	2.17/41.58 (30)		3.17/28.14 (50)			2.752/32.5 (60)	2.279/39.5 (45)	
1.93/47.04 (18)	3.66/24.3 (25)	1.894/48 (30)		2.50/35.88 (50)			2.806/31.86 (55)	1.611/57.12 (45)	
1.647/55.76 (14)		2.68/33.42 (20)					3.072/29.06 (50)	1.777/51.38 (40)	
1.75/52.22 (10)		4.06/21.88 (20)						1.979/45.8 (35)	
		2.52/35.60 (20)							
		2.37/37.94 (20)							
		2.24/40.22 (20)							
		2.19/41.18 (20)							

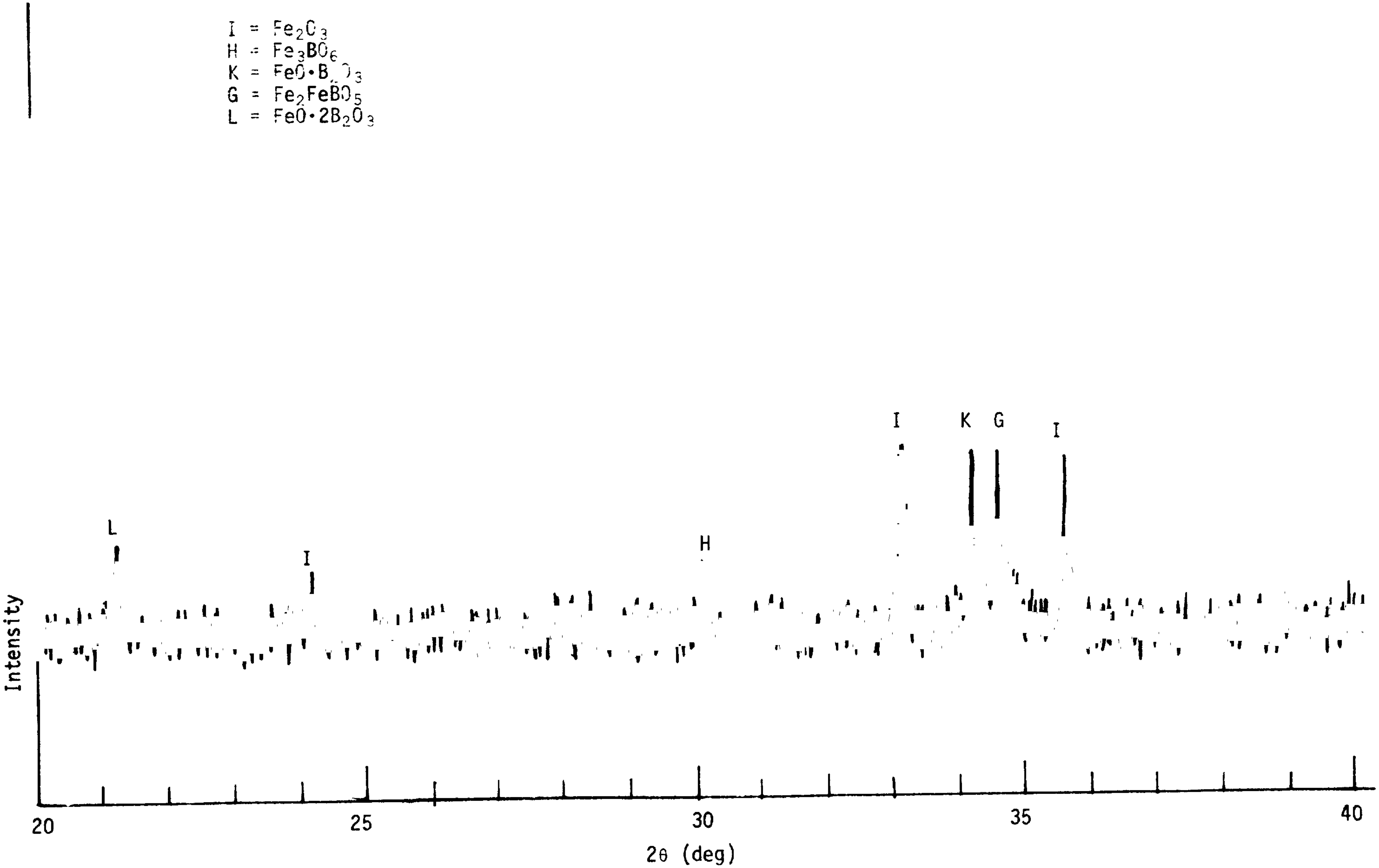

Figure 1 X-ray Diffraction Pattern of Splat Plate of 50B-1 Melt (1316°C - 7 Hrs.)

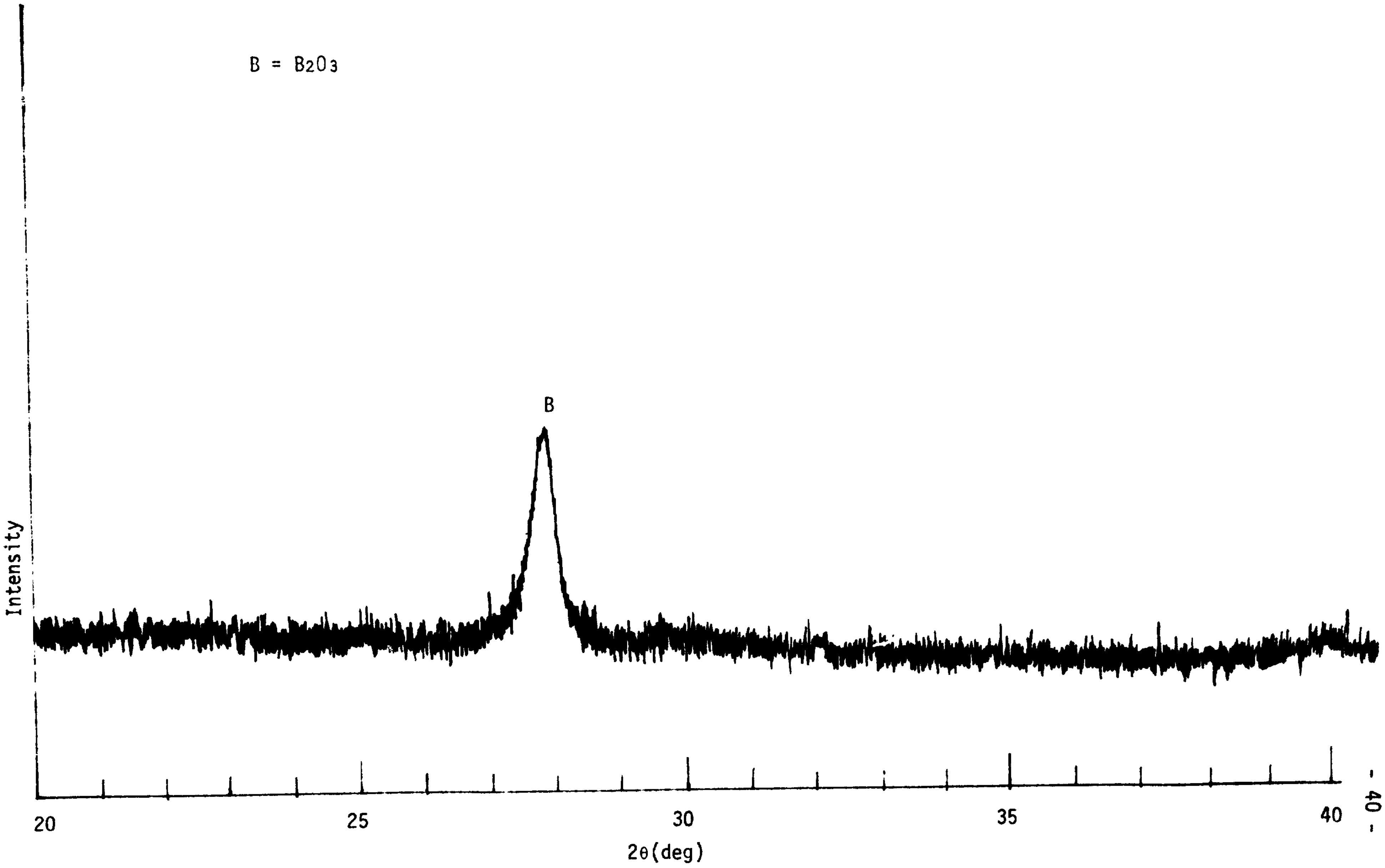

Figure 2 X-ray Diffraction Pattern of Splat Plate of 80B-1 Melt (1316°C-7 Hrs.)

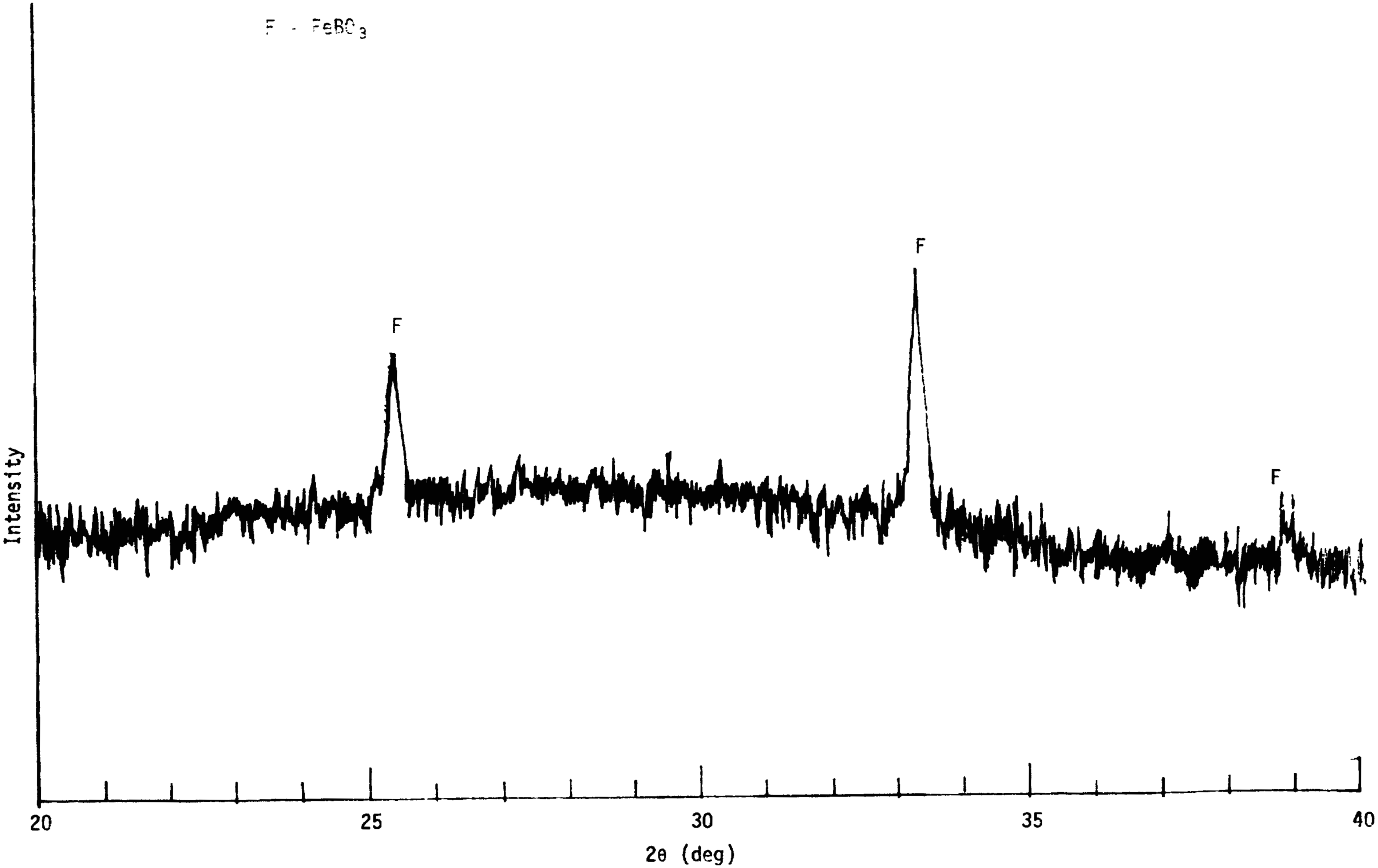

Figure 3 X-ray Diffraction Pattern of Crystallized Splat Plate of 83B-Bi-1 Melt (1200°C-4 Hrs.) at 680°C - 24 Hrs.

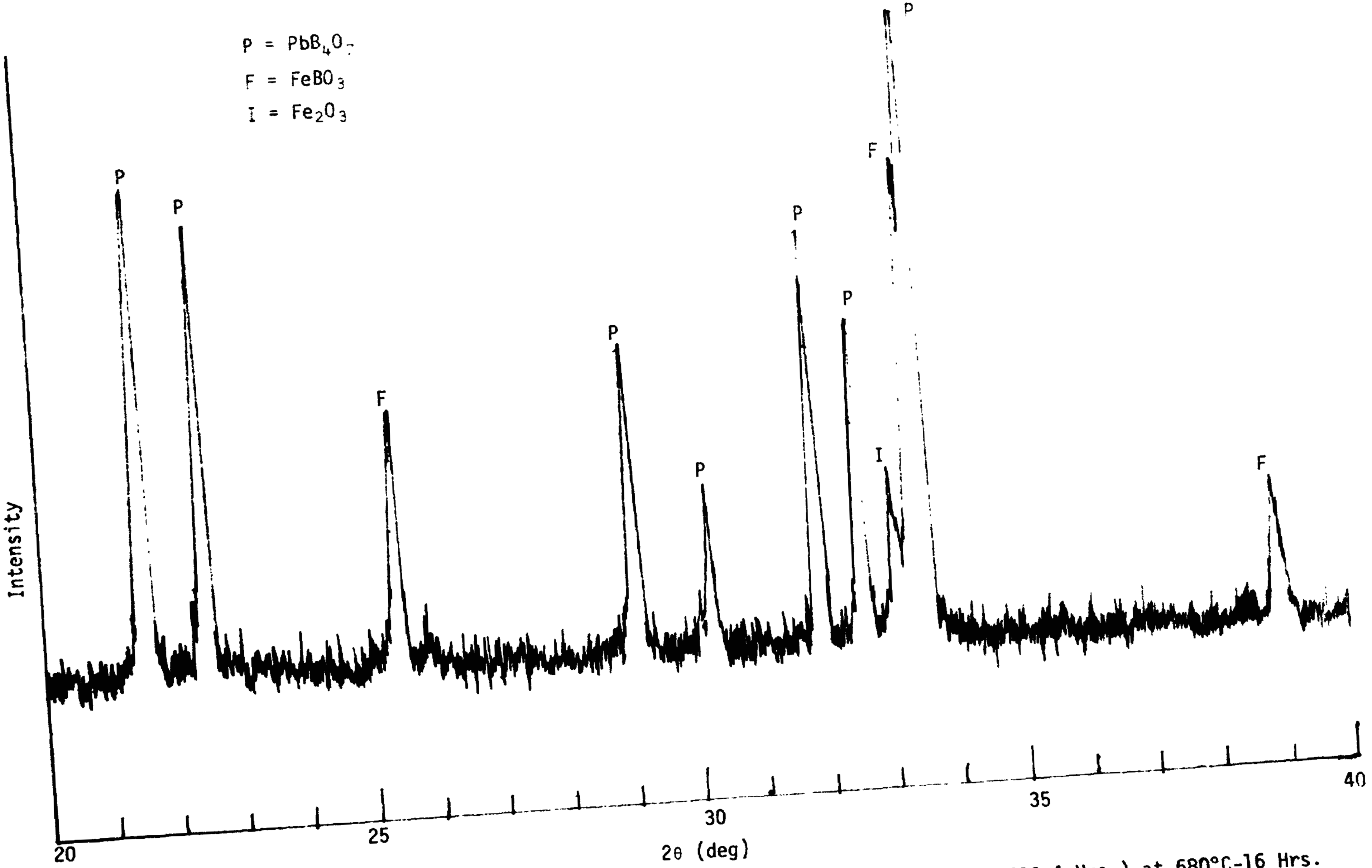

Figure 4 X-ray Diffraction Pattern of Crystallized Splat Plate of 83B-Pb-1 Melt (1200°C-4 Hrs.) at 680°C-16 Hrs.

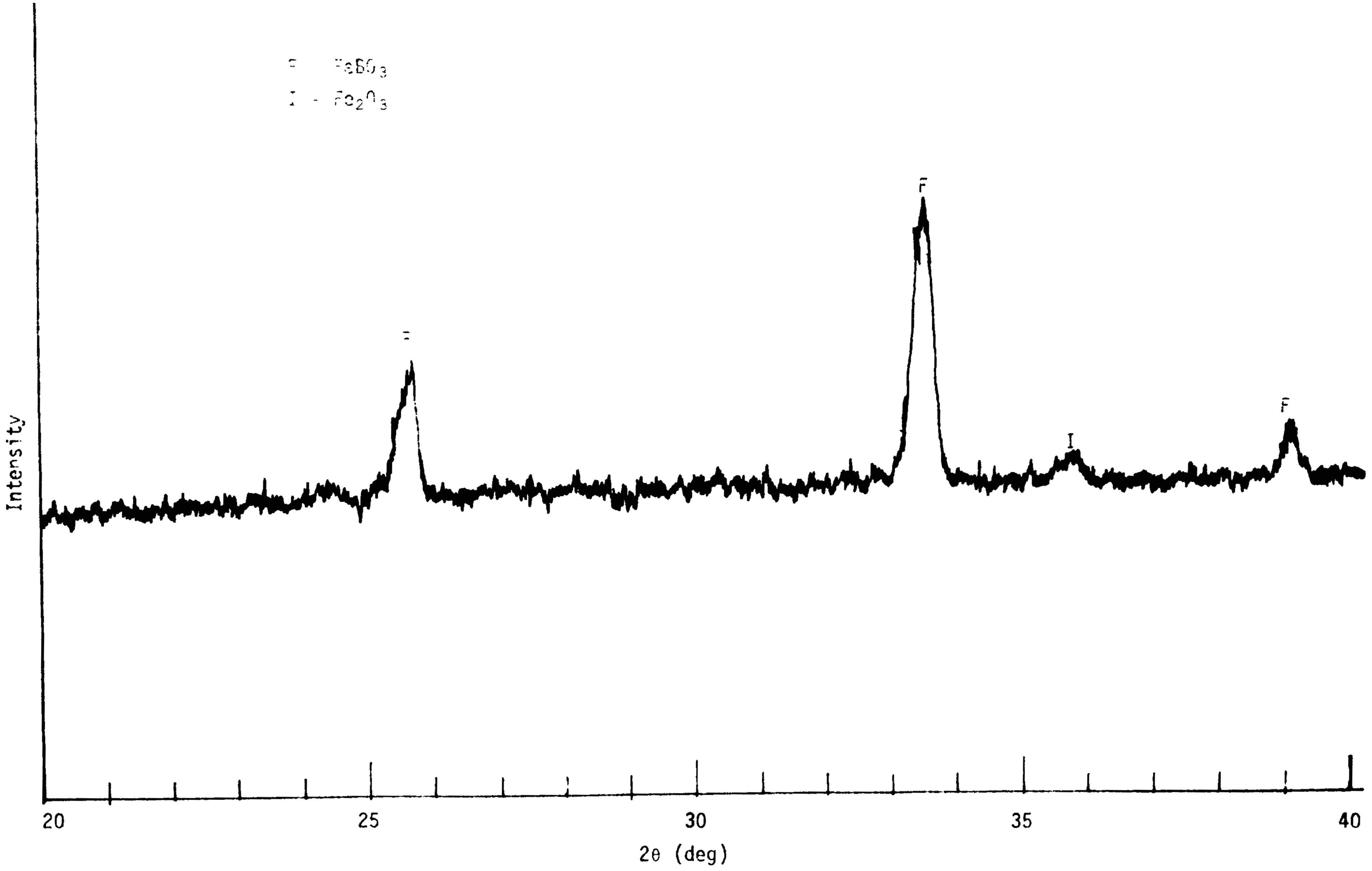

Figure 5 X-ray Diffraction Pattern of Crystallized Splat Plate of 50B-1 Melt (1316°C-7 Hrs.) at 721°C-4 days

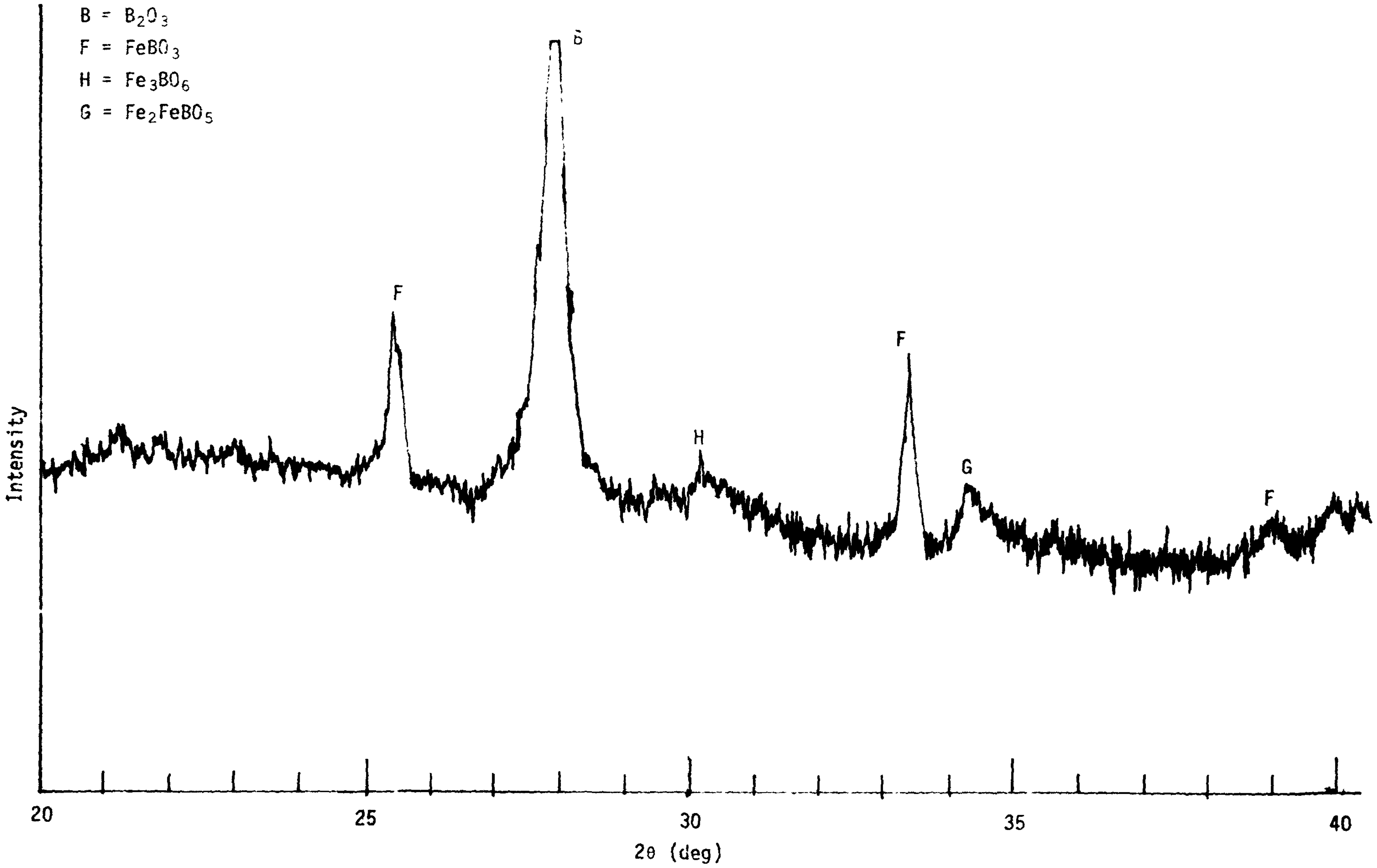

Figure 6 X-ray Diffraction Pattern of Crystallized Splat Plate of 80B-1 Melt (1316°C-7 Hrs.) at 721°C-4 Days

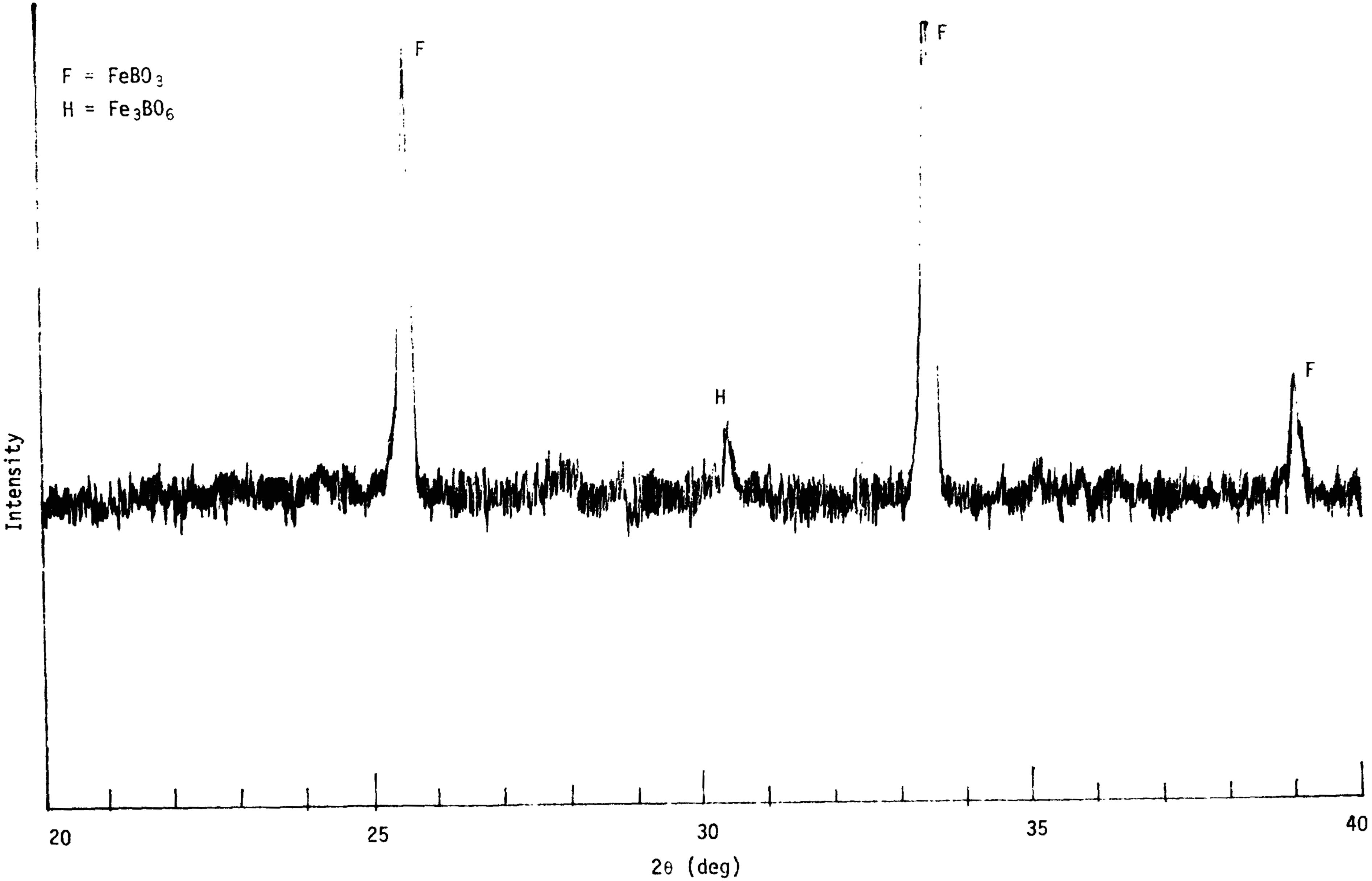

Figure 7 X-ray Diffraction Pattern of Crystallized Batch Material of 80B-4 at 680°C-4 Days

Appendix 1

Derivation for B_2O_3-Fe_2O_3 Classification

No. Corners Shared	Oxygen Coordination*	Charge Balance		Material Balance		
		Charge per Oxygen	Local Imbalance	Per Oxygen	No. of Oxygen	Overall
3	O"-2B	2	0	$O''B_{2/3}$	x = 3	B_2O_3
2	O"-2B	2	0	$O''B_{2/3}$	x = 6	B_4O_6
	O'-B+2Fe	2	0	$O'B_{1/3}Fe_{2/6}$	y = 3	$FeBO_3$
						FeB_5O_9
1	O"-2B	2	0	$O''B_{2/3}$	x = 3	B_2O_3
	O'-B+2Fe	2	0	$O'B_{1/3}Fe_{2/6}$	y = 6	$Fe_2B_2O_6$
						$Fe_2B_4O_9$
0	O'-B+2Fe	2	0	$O'B_{1/3}Fe_{2/6}$	y = 3	$FeBO_3$

*The coordinations were taken to be 3 for B, and 6 for Fe based upon the crystal structural information.